# Multi-angle Imaging SpectroRadiometer (MISR) On-Board Calibrator (OBC) In-Flight Performance Studies

Nadine L. Chrien, Carol J. Bruegge, and Robert R. Ando

***Abstract*—The Multi-angle Imaging SpectroRadiometer (MISR) consists of nine cameras pointing from nadir to an extreme of 70.5° in the view angle. It is a pushbroom imager with four spectral bands per camera. Instrument specifications call for each camera to be calibrated to an absolute uncertainty of 3% and to within 1% relative to the other cameras. To accomplish this, the MISR instrument utilizes an on-board calibrator (OBC) to provide updates to the instrument gain coefficients on a bimonthly basis (i.e., once every two months). Spectralon diffuse panels are used in the OBC to provide a uniform target for the nine MISR cameras to view. The radiometric scale of the OBC is established through the use of photodiodes. The stability of the MISR OBC system and its in-flight calibration are discussed in this paper.**

***Index Terms*—Calibration, photodiodes, radiometry.**

## I. Introduction

The Multi-angle Imaging SpectroRadiometer (MISR) on-board calibrator (OBC), illustrated in Fig. 1, consists of two Spectralon diffuse calibration panels, high quantum efficiency photodiodes (HQE), radiation-resistant photodiodes (referred to as PIN which derives from the diode architecture of stacked $p$, intrinsic, and $n$ doped layers), and a goniometer. The panels are deployed for calibration once every two months over the poles to reflect diffuse sunlight into the fields of view of the nine cameras that comprise the MISR instrument. The calibration data collection is timed so that the cameras will see a range of illumination, from sunrise (sunset at the South Pole) on the panel, to a view of the sun through a varying amount of earth atmosphere including atmosphere-free space. The photodiodes are used to measure the panel-reflected radiances, allowing the cameras to be calibrated using data covering the dynamic range of the sensors. The cameras' responses to the varying levels of incident radiance are fitted to provide pixel-by-pixel gain coefficients mapping camera digital number (DN) to observed radiance [1]. The fore–aft cameras are paired in a symmetrical arrangement and are set at fixed view angles. Each set of off-nadir cameras, fore or aft, views a single diffuse panel. The off-nadir cameras are referred to as Af/Aa, Bf/Ba, Cf/Ca, and Df/Da in order of increasing view angle relative to the earth's surface. There is also a nadir camera (An) that views both diffuse panels.

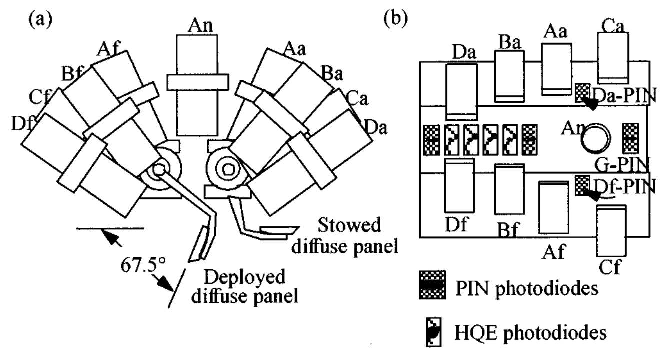


Fig. 1. Schematic of the MISR instrument showing the OBC. (a) South panel deployed and the north panel in its stowed position (the spacecraft flight direction is to the right with nadir being down). (b) Locations of the four HQE photodiode packages, the five PIN photodiode packages, and the nine cameras on the MISR optical bench (the spacecraft flight direction is toward the top of the page with nadir being into the page).

The MISR OBC was designed to provide a flat-field calibration of the MISR instrument and to provide a means of performing that calibration over much of the dynamic range of the instrument. The Spectralon diffuse panels were selected for their near-Lambertian and spectrally neutral reflectance properties to aid in the camera-to-camera and band-to-band relative calibrations of the MISR instrument. The HQE photodiodes were selected for use as detector standards to provide an absolute measure of the panel radiance. Due to concerns over the long-term stability of the NIR HQE photodiode, the more radiation resistant PIN photodiode detector standards were also incorporated into the design of the MISR OBC. The goniometer was included to monitor the panel reflectance as a function of angle in the along-track direction.

By monitoring the panels with the photodiode assemblies and through vicarious calibration using overflight campaign data, the performance of the MISR OBC may be evaluated. Of importance in the calibration of MISR are changes in the panels, changes in the diodes, and making use of the strengths of the vicarious calibration over the preflight calibration of the photodiodes to set the absolute radiometric scale of the OBC. This paper addresses the OBC studies that have been performed. The details of the vicarious calibration and its validation are covered in companion papers [1], [2].

Manuscript received September 20, 2001; revised April 11, 2002. This work was conducted at the Jet Propulsion Laboratory, California Institute of Technology, under contract with the National Aeronautics and Space Administration.

The authors are with the Jet Propulsion Laboratory, California Institute of Technology, Pasadena, CA 91109 USA (e-mail: Nadine.L.Chrien@jpl.nasa.gov).

Publisher Item Identifier 10.1109/TGRS.2002.801156.

## II. Description of the On-Board Calibrator

### A. Photodiodes

Both types of photodiode packages (PIN and HQE) consist of three main sections: a hermetically sealed assembly containing the photodiodes, an electronic assembly, and a precision baffle assembly that defines the étendue $(A\Omega)$ of the sensor [3]. The OBC photodiodes use the same filter designs as the MISR instrument; however, the filters come from different coating runs, and the out-of-band spectral responses differ due to the differing systems configurations [4]. The four MISR spectral bands are termed, respectively, Bands 1–4 or blue, green, red, and near-infrared (NIR) and are centered at 446, 558, 672, and 866 nm with equivalent bandwidths of 42, 29, 22, and 40 nm respectively (as determined from a solar-weighted, in-band moments analysis [5]).

*1) PIN Photodiode Packages:* A PIN photodiode package contains four diodes, each filtered to match one of the MISR spectral bands. Within the hermetic package, the filter is located directly over the diode with a small gap between the filter and the diode surface. The PIN photodiodes are radiation resistant.

There are five PIN photodiode packages on the MISR OBC: two of the PIN photodiodes are nadir-pointing; two point in the MISR D-camera directions, one forward and one aft; and one is mounted on the goniometer.

*2) HQE Photodiode Packages:* An HQE photodiode package contains within the hermetic package three photodiodes, arranged optically in series, in a light-trap configuration. A single spectral filter is bonded to the window of the hermetic package. Each HQE photodiode package is filtered to a single MISR spectral band. Two different detector designs were used in the construction of the HQE photodiode packages: one design favoring the NIR in responsivity and the other favoring the shorter wavelengths. The latter design, used for the blue, green, and red HQE photodiode packages, was shown to be as radiation resistant as the PIN photodiodes during proton radiation damage testing [3]. All of the HQE photodiode packages are nadir pointing.

### B. Goniometer

The goniometer is a mechanized device that characterizes the diffuse panel radiance as a function of angle. It does so in a plane that lies parallel to the spacecraft flight direction. A PIN photodiode package mounted to the goniometer arm swings through $\pm 60°$ to allow panel characterization appropriate to the along-track camera angles. (Note that a 58° view angle at the spacecraft results in a 70.5° view angle at the earth's surface, the difference being due to earth curvature.)

### C. Diffuse Panels

The diffuse panels are referred to as "north" and "south," which indicates at which pole the panel is deployed. The MISR nadir and aft cameras view the north panel at the North Pole, while the MISR nadir and forward cameras view the south panel at the South Pole. The panels are made of Spectralon, a material chosen for its high, near-Lambertian reflectance [6].

The bidirectional reflectance factor (BRF) of a test sample of the panel material was characterized in laboratory experiments at source illumination angles of 40°, 45°, 50°, and 55° to the panel normal which encompasses the incident solar angles onto the panels during calibration sequences [7]. The source azimuth in the laboratory setup was 0°. A test sample was used, as the panels themselves were too large for the laboratory setup. This measured BRF database is used to correct for departure from Lambertian behavior when camera calibration is done. The detector view angle, sun angle with respect to the panel normal, and the difference between the sun and detector azimuth angles between the 1504 elements $\times$ 4 bands of an MISR camera and the OBC photodiodes are taken into account when accessing the BRF database and computing the camera radiance. Due to the solar azimuth angles on the diffuse panels and the OBC geometry, the cameras and photodiodes view the forward scatter region of the BRF. The nadir viewing diodes actually view the diffuse panels at approximately $-67°$ from the panel normal, while the D-photodiodes view the panels at an angle of about $-9.5°$ from the panel normal as can be seen in Fig. 1(a). The solar zenith angles on the diffuse panels during acquisition of data used in calibration are typically in the range of 45° to 55° throughout the course of the year, and for a given calibration acquisition, the solar zenith angle on the panel changes by about 4°, while the solar azimuth angle on the panel changes by only about 1°. The exact angles during a calibration sequence vary with the date of calibration.

## III. Use of the On-Board Calibrator

### A. Photodiodes Measure Panel-Reflected Radiance

The OBC photodiodes are used to measure the panel-reflected radiance seen by the MISR cameras during calibration. The radiance measured by a photodiode package in units of $\mathrm{W\,m^{-2}\,sr^{-1}\,\mu m^{-1}}$ is given by

$$L^{\mathrm{std,OBC}} = \frac{1.2395\ [\mathrm{W}\ \mu\mathrm{m\,Amp}^{-1}] \cdot i \cdot E_0^{\mathrm{std}}}{(A\Omega\Re) \cdot k}, \qquad \Re = \int_{0.2\ \mu\mathrm{m}}^{1.2\ \mu\mathrm{m}} E_{0,\lambda} R_\lambda \lambda \partial\lambda \tag{1}$$

where

- $i$ photodiode current (Amperes);
- $A\Omega$ étendue for the OBC photodiode $(\mathrm{m}^2\ \mathrm{sr})$;
- $E_0^{\mathrm{std}}$ standardized response weighted exoatmospheric solar irradiance at 1 astronomical unit (AU) [5] $(\mathrm{W\,m^{-2}\ \mu m^{-1}})$;
- $k$ photodiode calibration factor;
- $R_\lambda$ the spectral response function of the photodiode;
- $E_{0,\lambda}$ spectral exoatmospheric solar irradiance function $(\mathrm{W\,m^{-2}\ \mu m^{-1}})$;
- $\Re$ solar-weighted detector response $(\mathrm{W\,m^{-2}\ \mu m})$.

### B. Camera Radiance is Computed Using BRF Database

The radiance for a given detector element, $L^{\mathrm{std}}(\theta_i, \phi_i; \theta_r^p, \phi_r^p)$ is computed as

$$L^{\mathrm{std,OBC}}\left(\theta_i, \phi_i; \theta_r^{\mathrm{OBC}}, \phi_r^{\mathrm{OBC}}\right) \cdot \frac{\mathrm{BRF}\left(\theta_i, \phi_i; \theta_r^p, \phi_r^p\right)}{\mathrm{BRF}\left(\theta_i, \phi_i; \theta_r^{\mathrm{OBC}}, \phi_r^{\mathrm{OBC}}\right)}. \tag{2}$$

$\theta_r^p$ and $\phi_r^p$ are the reflected zenith and azimuth angles, respectively, as viewed by a given detector element $p$.

### C. Camera Gain Coefficients are Derived

The analysis of the OBC data begins with the assumption that the instrument response can be modeled as

$$DN - DN_0 = G_0 + G_1 L^{\mathrm{std,OBC}} + G_2 L^{\mathrm{std,OBC}^2} \tag{3}$$

where

- $L^{\mathrm{std,OBC}}$ radiance for a detector element ($\mathrm{W\,m^{-2}\ sr^{-1}\ \mu m^{-1}}$);
- $DN$ camera output digital number;
- $DN_0$ DN offset, unique for each line of data;
- $G_0, G_1, G_2$ gain coefficients which provide the radiometric calibration of a specific pixel.

The gain coefficients are computed for each of the 1504 active pixel elements per line array and for each of the nine cameras and four spectral bands through linear regression using (3). The photodiodes in conjunction with the BRF of the diffuse panels are used to determine the spectral radiance incident on each camera detector element.

## IV. In-Flight Performance of the OBC

### A. Photodiode Packages

As a validation of the radiance measured by the OBC, we can also predict the radiance reflected into an OBC detector (either a photodiode package or camera detector element) in units of $\mathrm{W\,m^{-2}\ sr^{-1}\ \mu m^{-1}}$ through knowledge of the solar spectral irradiance, the sun angle on the panel, the panel reflectance, and the mean earth–sun distance; however, this method does not account for the possibility of extraneous illumination on the panel. Two potential sources of extraneous illumination that have been identified are 1) that the MISR radiator plates may inadvertently be in the fields-of-view of the panels when the panels are deployed and 2) earthshine [8]. Despite the potential for underrepresenting the panel radiance, the prediction allows for stability studies, by taking into account differences in the incident irradiance due to changes in sun angle and sun–earth distance with time. The equation for predicted panel radiance is simply

$$L^{\mathrm{std,OBC}}_{\mathrm{predicted}} = \frac{\cos(\theta_i) \cdot \mathrm{BRF}\left(\theta_i, \phi_i; \theta_r^{\mathrm{OBC}}, \phi_r^{\mathrm{OBC}}\right) \cdot E_0^{\mathrm{std}}}{\pi R^2} \tag{4}$$

where

- $\theta_i, \phi_i$ incident zenith and azimuth angles, respectively, with respect to the panel normal;
- $\theta_r^{\mathrm{OBC}}$, $\phi_r^{\mathrm{OBC}}$ reflected zenith and azimuth angles, respectively, as viewed by a given photodiode;
- BRF preflight measured bidirectional reflectance function database for the panel;
- $R$ geocentric distance between the sun and earth in AU.

Upon examination of the first in-flight OBC data acquired, a comparison of the measured diode radiance to the predicted diode radiance was made. It was determined that the preflight characterizations of the photodiode radiometric responses were flawed. A difference in radiance between the HQE and PIN photodiodes of approximately 10% was noted (almost 20% in the NIR) as well as unexpected variance in the radiance from band to band (Fig. 2). The early data using the preflight calibrations show a range in the HQE radiances of 15% from band to band. The spread in the OBC preflight radiance leads us to suspect errors in the preflight diode characterization. It is believed that inaccuracy in the procedure to correct for the out-of-band spectral response of the photodiodes is responsible for the discrepancies.

As expected, the NIR HQE photodiode is exhibiting a decline in responsivity with time due to radiation damage. The other photodiodes are relatively stable, with the exception of the green bands. This was an unexpected occurrence and is attributed to the green filters themselves; however, as will be discussed later, all diodes are calibrated to the blue HQE prior to the camera calibration, so this degradation is mitigated. The MISR cameras also show a decline in responsivity with time. In Fig. 3, the ratio of measured radiance using the preflight calibration coefficients to the predicted radiance for the nadir (An) camera is shown. The other MISR cameras give similar results. The green bands of the cameras do not exhibit any more degradation than the other bands. The camera response across all bands has changed by about 7% from the time the MISR cover opened in February 2000 to May 2000, with the most rapid change occurring in the first couple months. The cameras all share a common design, and it is thought that the change in response is due to a reduction in throughput caused by contamination and the radiation environment on-orbit.

Due to the spread in the OBC preflight radiance, it was decided to use a single photodiode package as the standard to which the others would then be calibrated. The blue HQE was selected for this purpose, due to its stability and its close agreement with the predicted radiance. To calibrate the photodiodes, we assume the panel reflectance is the same for all four MISR bands in order to tie all spectral bands of the other photodiodes to the single spectral band of the blue HQE. Also, as the photodiodes see different physical locations on the diffuse panels, the panel reflectance needs to be spatially uniform. Preflight testing of MISR test pieces and other Spectralon samples has shown the reflectance of Spectralon to be spectrally neutral and highly repeatable [7], [9]. If the two aforementioned conditions hold, then the ratio of one diode current to another should equal the ratio of the étendue-response products $A\Omega\Re$, since the radiance observed by a photodiode is proportional to its current

$$\begin{aligned}\frac{i_2}{(A\Omega\Re)_2 \cdot k_2} &= \frac{L_2^{\mathrm{std,OBC}}}{E_{0,2}^{\mathrm{std}}} = \frac{L_1^{\mathrm{std,OBC}}}{E_{0,1}^{\mathrm{std}}} \\ &= \frac{i_1}{(A\Omega\Re)_1 \cdot k_1} \Rightarrow \frac{i_2}{i_1} = \frac{(A\Omega\Re)_2 \cdot k_2}{(A\Omega\Re)_1 \cdot k_1}\end{aligned} \tag{5}$$

$$\begin{aligned}k_{\mathrm{diode,band}} &= \frac{i_{\mathrm{diode,band}}}{i_{\mathrm{HQE,blue}}} \cdot \frac{(A\Omega\Re)_{\mathrm{HQE,blue}}}{(A\Omega\Re)_{\mathrm{diode,band}}} \\ &\quad \cdot k_{\mathrm{HQE,blue}}\end{aligned} \tag{6}$$

$$\begin{aligned}k_{D\text{-diode,band}} &= \frac{i_{D\text{-diode,band}}}{i_{\mathrm{goni,band}}^{@D\text{-angle}}} \cdot \frac{(A\Omega\Re)_{\mathrm{goni,band}}}{(A\Omega\Re)_{D\text{-diode,band}}} \\ &\quad \cdot k_{\mathrm{goni,band}}.\end{aligned} \tag{7}$$

The calibration factors $k_{\mathrm{diode,band}}$ for the nadir pointing diodes are computed using the blue HQE diode as the standard (6). The D-diodes are calibrated to the blue HQE diode using

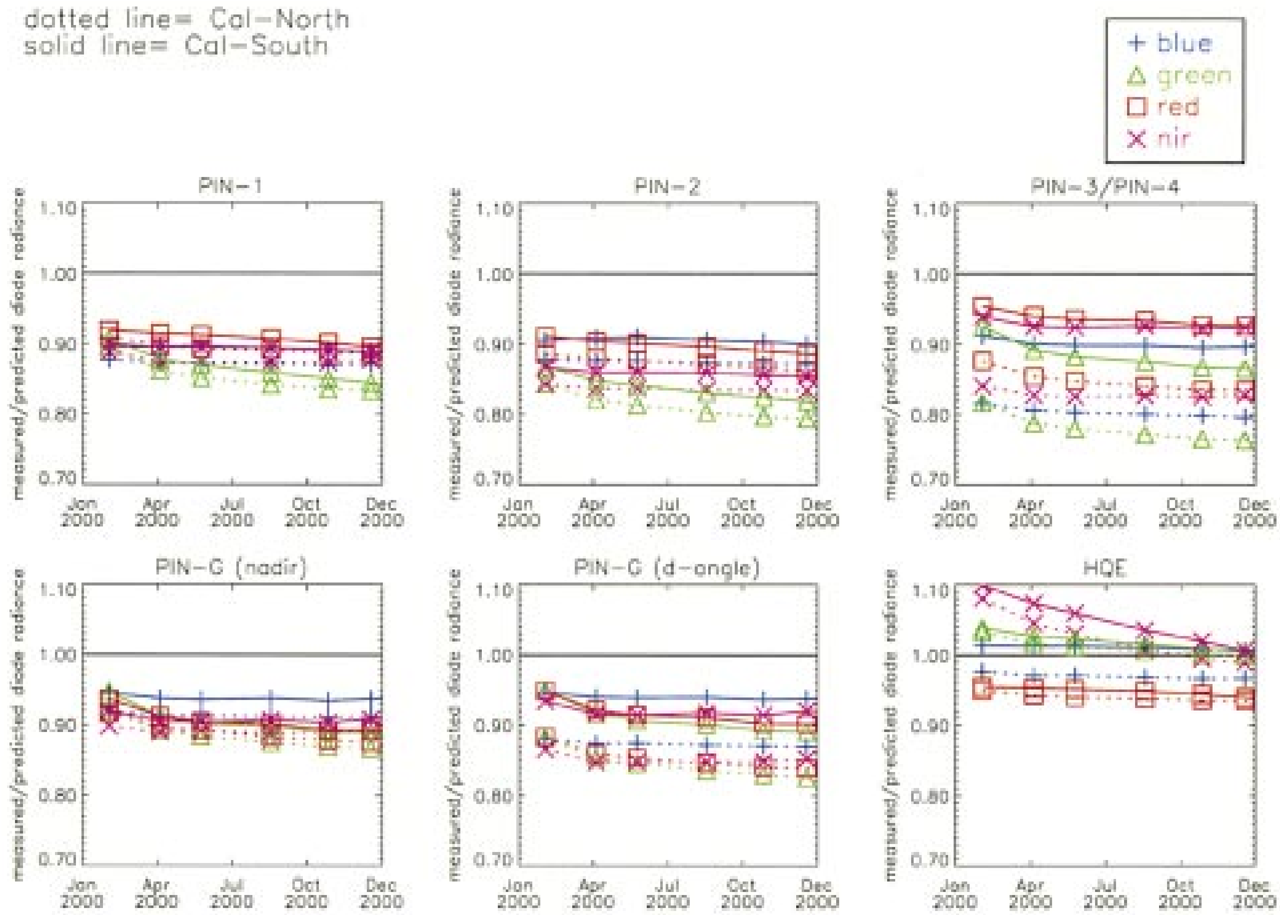


Fig. 2. Ratio of measured to predicted radiance for the OBC photodiodes, nadir packages (HQE, PIN-1, and PIN-2), D-forward package (PIN-3), D-aft package (PIN-4), and goniometer photodiode package (PIN-G) for all bands and both north (solid) and south (dotted) diffuse panels using the preflight OBC calibrations over time. The figure illustrates the stability of the blue HQE and diffuse panel reflectance, as well as the discrepancies in the preflight characterizations of the photodiodes.

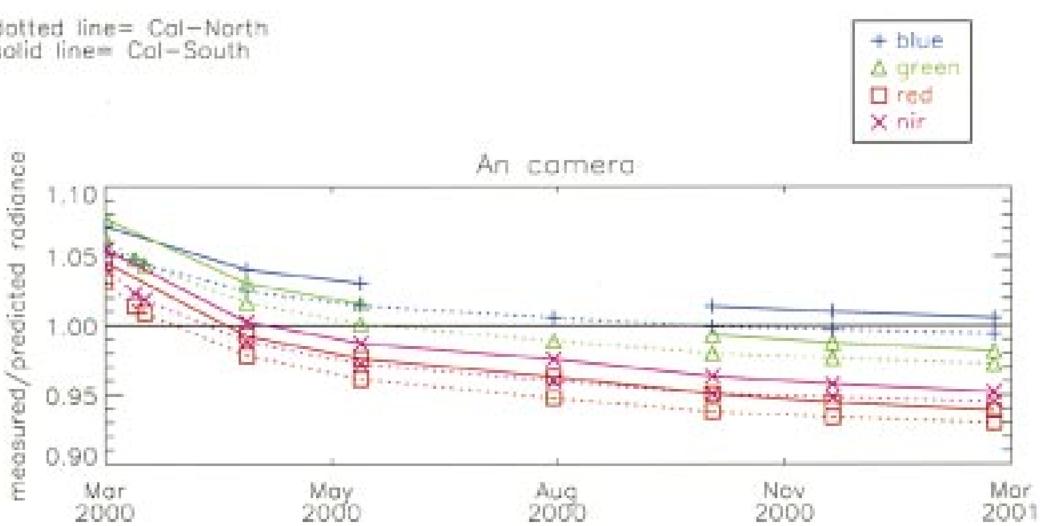


Fig. 3. Ratio of measured to predicted radiance for the A-nadir camera for all bands and both north (solid) and south (dotted) diffuse panels using the preflight camera calibration coefficients over time. The figure illustrates the bias between north (solid) and south (dotted) panels and the tailing off of the degradation in camera responsivity with time.

the goniometer as a transfer standard. The goniometer calibration factors are computed using the blue HQE diode as the standard by finding the average current when the goniometer position is nadir pointing. The D-diode bands are then calibrated to the goniometer diode bands using the average current when the goniometer is pointing in the D-diode direction (7). The calibration factors are computed using the average currents during the time the goniometer is running. The goniometer is run for a short portion of the calibration sequence when the illumination on the panel is atmosphere-free. It is not possible to use the goniometer to measure the incoming radiance with angle during the sunrise/sunset portion of the calibration sequence, as the light levels are changing too rapidly. The fixed diodes are required for calibration of the cameras using data acquired over the dynamic range of each camera.

The absolute radiometric scale used for MISR calibration is set, based on the value chosen for the blue HQE calibration factor $k_{\mathrm{HQE,blue}}$. This value was set to 0.91, based upon the June 2000 Lunar Lake vicarious calibration experiment [1]. The vicarious calibration experiment indicates that the predicted radiance from the panel given in (4) is too low. The diode preflight calibrations are suspect, due to the resultant range of radiances. The most likely explanation is a secondary source of illumination onto the panels, such as from reflections off the MISR radiator plates or from surrounding structures on the spacecraft or perhaps earthshine [8].

All the OBC photodiodes, except the D-aft PIN, are calibrated while viewing the south panel. The D-aft PIN photodiode only views the north panel, so it is calibrated through a transfer from the goniometer PIN photodiode that is calibrated while viewing the south panel. The south panel was chosen for calibration because it more closely resembles the BRF database.

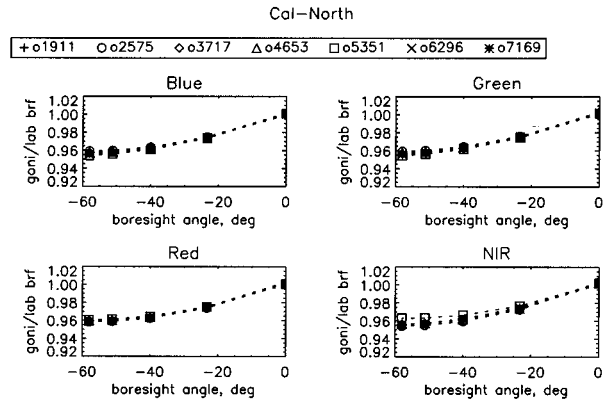


Fig. 4. North panel relative reflectance with angle, normalized to value at nadir as measured by the goniometer compared to the BRF database. A departure of 4% across the MISR aft camera angles is seen. Data from six OBC experiments covering 12 months shows the reflectance is different from the database but stable.

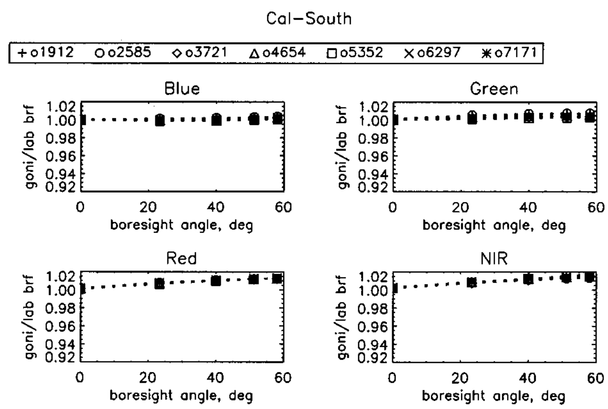


Fig. 5. South panel relative reflectance with angle, normalized to value at nadir as measured by the goniometer compared to the BRF database. Data from six OBC experiments covering 12 months shows the stability of the panel reflectance and generally good agreement with the BRF database.

## *B. Diffuse Panels*

The relative panel reflectance with angle can be measured using the goniometer. The goniometer data show the angular reflectance to be stable over time; however, when the angular reflectance data are compared to the measured BRF database, as in Figs. 4 and 5, a discrepancy between the north and south panels is found. The BRF of the south panel matches the BRF database fairly well with at most a 1.5% difference with angle in the red and NIR bands. The BRF of the north panel departs from the BRF database by about 4% in all four spectral bands across the range of MISR camera boresight angles. This difference in the panel BRF is also seen in Fig. 3, in that the ratio of measured to expected radiance for each diode differs for the north and south panels. Due to the stability of the relative panel reflectance with angle over time, it is most likely that the angular reflectance of the north panel never matched that of the test piece from which the laboratory-measured BRF database was derived. The flight panels were not measured directly, and the test piece was made from the same material lot as the flight panels; however, the panels were fabricated individually in their respective trays. It is supposed that some variation in manufacturing is responsible. The key factor in the calibration of MISR is that the diffuse panels are stable.

The goniometer only provides measurements along one dimension of the diffuse panels and so cannot be used to completely characterize the panel BRF. Fortunately, the BRF of Spectralon as viewed in the cross-track dimension of the MISR cameras is slowly varying. The error in computed radiance introduced by the departure of the actual BRF from the BRF database can be reduced by using the radiance from the D-angle PIN photodiode to calibrate the off-nadir cameras and the radiance from the nadir-pointing $-y$ PIN photodiode to calibrate the nadir camera. The BRF database is still used to compute the radiance for a given detector element; however, the BRF correction is smaller. Also, the BRF changes less at the D-angle with changing sun angle. The bias between the forward and aft cameras caused by the fact that the forward cameras are calibrated with the south panel and the aft cameras are calibrated with the north panel are further reduced by scaling the BRF from the BRF database when the north panel is deployed. Scaling factors were computed at each of the five MISR camera boresight angles for the north panel such that the goniometer-to-lab BRF ratio equaled that of the corresponding ratio from the blue band of the south panel. They are 0.928, 0.930, 0.935, 0.948, and 0.973 for the Da, Ca, Ba, Aa, and An cameras, respectively. A single scaling factor based on boresight angle is applied to the cross-track BRF derived

TABLE I
MISR OBC ERROR SOURCES

| Parameter | Radiometric uncertainty, % Abs. | Cam. | Band | Pixel |
|---|---|---|---|---|
| VC radiance | 3 | | | |
| VC to blue HQE transfer | 2 | | | |
| Blue HQE temporal stability | 1 | | | |
| Blue HQE to operational photodiodes | 0.5 | 0.5 | 0.5 | |
| Camera to photodiode view angle BRF ratio | 1 | 1 | | |
| Diffuse panel spatial uniformity | 0.5 | 0.5 | 0.5 | 0.5 |
| Diffuse panel spectral uniformity | | | 1 | |
| Diode Signal-to-Noise Ratio | 0.1 | 0.1 | 0.1 | 0.1 |
| Point Spread Function effects | 0.1 | 0.1 | 0.1 | 0.1 |
| Root-Sum-Square | 3.9 | 1.2 | 1.2 | 0.5 |

from the BRF database. The BRF correction relative to the photodiode being used for calibration is of primary interest. These ratios are 1.0, 1.002, 1.008, 1.022, and 1.0 for the Da, Ca, Ba, Aa, and An cameras using the D-aft PIN photodiode to calibrate the off-nadir aft cameras and the $-y$ PIN photodiode to calibrate the An camera. This method appears to reduce the bias between the aft and forward camera calibration [1].

## V. MISR Calibration Uncertainties

The absolute calibration of the OBC is tied to the June 11, 2000 vicarious calibration experiment (VC) described in detail elsewhere [1], [2]. The VC radiance computation is the dominant error in the OBC uncertainties but does not affect the camera, band, or pixel relative radiometric uncertainty. Uncertainty associated with the blue HQE temporal stability is 1%, based on vicarious calibration experiments occurring on a yearly basis. The transfer of radiance from the blue HQE photodiode to the other OBC photodiode standards is believed to be accurate with potential errors resulting from temporal sampling differences. Only the relative panel bidirectional reflectance factors (BRF) are involved in the correction for photodiode to camera view angle, so that correction also has a low uncertainty. The panel spatial uniformity is good, or the MISR images would show artifacts when processed with the gain coefficients derived on-orbit. The photodiodes have high signal-to-noise ratios, so they contribute little to the calibration uncertainty; and the diffuse panels, while finite in extent, were sized to minimize point spread function effects when viewed by the cameras. These error sources and their contributions to the MISR calibration uncertainties are summarized in Table I.

## VI. Conclusions

The MISR on-board calibrator provides a flat field calibration of the nine MISR cameras in-flight. The stability of the Spectralon diffuse panels combined with the stability of the OBC photodiodes, the blue HQE in particular, has allowed the faulty preflight calibration of the OBC to be overcome.

The effect of the changes in the responsivity of the MISR cameras over time is not a concern because the MISR OBC allows for the in-flight calibration of the cameras at regular intervals. The observed changes in the responsivity of the MISR cameras have also become smaller with time.

The goniometer has proven instrumental in determining the major contributor to a fore/aft camera bias and also in allowing the transfer calibration from the nadir, blue HQE diode to the D-diodes. The ability to use the D-diodes in calibrating the off-nadir cameras will help to minimize camera-to-camera relative calibration errors, as the panel BRF changes less with sun angle at the D-angle and since smaller relative BRF corrections are required between the D-diodes and the off-nadir cameras.

The MISR on-board calibrator is a crucial part of the overall calibration of the MISR instrument, particularly for the relative calibrations. The absolute calibration scale depends primarily on the vicarious calibration. It is possible that further refinements in the calibration procedures and scene-dependent corrections, which would apply to the vicarious calibration but not to the OBC data, will allow further reductions in the calibration uncertainties [1].

## Acknowledgment

The authors would like to thank the numerous people involved in the design, fabrication, characterization, and operation of the MISR instrument and its data systems.

## References

[1] C. Bruegge, N. Chrien, R. Ando, D. Diner, M. Helmlinger, W. Abdou, and K. Thome, "Early validation of Multi-angle Imaging SpectroRadiometer (MISR) radiometric scale," *IEEE Trans. Geosci. Remote Sensing*, vol. 40, pp. 1477–1492, July 2002.

[2] W. Abdou, C. Bruegge, M. Helmlinger, J. Conel, S. Pilorz, and B. Gaitley, "Vicarious calibration experiment in support of the Multi-angle Imaging SpectroRadiometer," *IEEE Trans. Geosci. Remote Sensing*, vol. 40, pp. 1500–1511, July 2002.

[3] C. Jorquera, V. Ford, V. Duval, C. Bruegge, and R. Korde, "State of the art radiometer standards for NASA's earth observing system," in *Conf. Proc. IEEE Aerosp. Appl.*, Feb. 1995.

[4] R. Korechoff, D. Diner, D. Preston, and C. Bruegge, "SpectroRadiometer focal-plane design considerations: Lessons learned from MISR camera testing," *EUROPTO/ SPIE*, vol. 2538, pp. 104–116, Sept. 1995.

[5] C. Bruegge, V. Duval, N. Chrien, R. Korechoff, B. Gaitley, and E. Hochberg, "MISR prelaunch instrument calibration and characterization results," *IEEE Trans. Geosci. Remote Sensing*, vol. 36, pp. 1186–1198, July 1998.

[6] C. Bruegge, D. Diner, and V. Duval, "The MISR calibration program," *J. Atmos. Ocean. Technol.*, vol. 13, no. 2, pp. 286–299, Apr. 1996.

[7] C. Bruegge, N. Chrien, and D. Haner, "A spectralon BRF data base for MISR calibration applications," *Remote Sens. Environ.*, vol. 77/3, pp. 352–364, Sept. 2001.

[8] J. Palmer, "Stray light effects on calibrations using a solar diffuser," *SPIE*, vol. 1493, pp. 143–154, 1991.

[9] E. Early, P. Barnes, B. Johnson, J. Butler, C. Bruegge, S. Biggar, P. Spyak, and M. Pavlov, "Bidirectional reflectance round-robin in support of the earth observing system program," *Amer. Meteorol. Soc.*, pp. 1077–1091, Aug. 2000.

**Nadine L. Chrien** received the B.S. degree in engineering in the field of systems science from the School of Engineering and Applied Sciences, University of California, Los Angeles, and the M.S. degree in optical sciences from the University of Arizona, Tucson.

She is currently with the Jet Propulsion Laboratory (JPL), Pasadena, CA, as a System Analyst for MISR and is currently working as part of the MISR In-Flight Radiometric Calibration and Characterization team on algorithm development. Prior to her work on MISR, she worked on the Mars Observer Pressure Modulator Infrared Radiometer (PMIRR) alignment, target simulator, and calibration monochromator systems.

**Carol J. Bruegge** received the B.A. and M.S. degrees in applied physics from the University of California, San Diego, in 1978 and the M.S. and Ph.D. degrees in optical sciences from the University of Arizona, Tucson, in 1985.

Currently, she is a Co-Investigator on the Multi-angle Imaging SpectroRadiometer (MISR) project and serves as the Calibration Scientist for that NASA Earth Observing System (EOS) instrument. Her experience is principally in the area of terrestrial remote sensing, calibration of remote sensing sensors, radiative transfer, and use of ground-truth measurements for validation and calibration of airborne and on-orbit sensors. She has been with the Jet Propulsion Laboratory, California Institute of Technology, Pasadena, since 1985 and has been involved with the absolute radiometric calibration of the Landsat Thematic Mapper, AirMISR, and Airborne Visible and Infrared Imaging Spectrometer (AVIRIS) sensors. She has also provided for the flight qualification of Spectralon, a diffuse material now used on-orbit for the radiometric calibration of sensors. Previously, she has been a Principal Investigator in the First International Land Surface Climatology Program Field Experiment (FIFE), a NASA ground-truth experiment.

**Robert R. Ando** received the B.S. degree in mechanical engineering from Duke University, Durham, NC, in 1973 and the M.S. degree in oceanography from Scripps Institution of Oceanography, La Jolla, CA, in 1978.

He has been with the Jet Propulsion Laboratory, Pasadena, CA, since 1996, providing software integration and test support and validating the radiometric calibration for the Multi-angle Imaging SpectroRadiometer (MISR) instrument.